

CIP/multi-moment finite volume method with arbitrary order of accuracy¹

Feng Xiao^{a,*}, Satoshi Ii^{a,b}

^aDepartment of energy sciences, Tokyo Institute of Technology, 4259 Nagatsuta, Midori-ku, Yokohama, 226-8502, Japan

^bCurrent address: Department of Mechanical Science & Bioengineering, Osaka University, Toyonaka, Osaka, 560-8531, Japan

Abstract

This paper presents a general formulation of the CIP/multi-moment finite volume method (CIP/MM FVM) for arbitrary order of accuracy. Reconstruction up to arbitrary order can be built on single cell by adding extra derivative moments at the cell boundary. The volume integrated average (VIA) is updated via a flux-form finite volume formulation, whereas the point-based derivative moments are computed as local derivative Riemann problems by either direct interpolation or approximate Riemann solvers.

Keywords: High order scheme, finite volume method, multi-moment, fluid dynamics, derivative Riemann problem, conservation

1. Introduction

The multi-moment concept underlying the CIP method (Cubic-Interpolated Pseudo-particle or Constrained Interpolation Profile)[16] provides a general methodology to construct numerical schemes with great flexibility. One of the major outcome from the practice so far to implement the multi-moments in computational fluid dynamics is that we can build high order schemes on a relatively compact grid stencil using multi-moments, and these moments can be carried forward in time separately by completely different numerical approaches.

Some schemes have been developed for practical use based on VIA and SIA (Surface-Integrated Average) [13][14] and on VIA and PV (Point Value) [3][4]. The later is much more suitable for unstructured or other complex computational grids where a point-wise local Riemann problem can be posed at any specified point to update the PV. It is found that increasing the number of the PVs is a simple way to get higher order schemes. We have devised and verified the schemes up to 4th order on 2D triangular unstructured grid for both scalar and system conservation laws by employing both VIA and PV moments. On the other hand, making use of the first derivative at the cell boundary as another moment has been ever used in the so-called CIP-CSL4(CIP-Conservative Semi-Lagrangian with 4th order polynomial) advection scheme [8].

We in this paper explore further the possibility to construct conservative CIP/multi-moment formulation of arbitrary order over single cell using more derivative moments. The spatial reconstruction based on multi-moments is described in section 2. The numerical formulation for scalar hyperbolic conservation law is presented in section 3. The extension to Euler equations is discussed in section 4. Section 5 ends the paper with a few conclusion remarks.

2. The multi-moment spatial reconstruction

The essential point in high resolution scheme is how to reconstruct the interpolation function to find the numerical flux at the boundary of each grid cell. Among the most widely used are, for example, the MUSCL scheme [12],

¹This paper was published in Proceedings of the 12th Computational Engineering Conference of Japan Society for Computational Engineering and Science (JSCES) Vol.12, May 22-24, 2007, Tokyo. Part of the contents were also published in a Japanese monograph *Computational Fluid Dynamics*, ISBN 978-4-339-04597-0, publish by Coronasha, 2009.

*Corresponding author: Feng Xiao, xiao@es.titech.ac.jp

the ENO scheme[2] and the WENO scheme [5]. In all of these schemes the interpolation is based only on the cell-averaged values of the physical field to be reconstructed. In this section, we describe a numerical interpolation that makes use of not only the volume-integrated average over each mesh cell but also the derivatives at the cell boundary. We call the present formulation the “multi-moment” reconstruction to distinguish it from the aforementioned ones which should be more properly refer to as the “single-moment” reconstruction.

We consider a physical field variable $\phi(x)$ over a one-dimensional domain divided into control volumes (mesh cells) $[x_{i-1/2}, x_{i+1/2}]$; $i = 1, 2, \dots, I$.

There is a flexibility in choosing the discretised moments for field variable $\phi(x, t)$. The primary moment of the finite volume method is the volume-integrated average (VIA) over each mesh cell

$$\overline{\phi}_i = \frac{1}{\Delta x_i} \int_{x_{i-1/2}}^{x_{i+1/2}} \phi(x, t) dx \quad (1)$$

where $\Delta x_i = x_{i+1/2} - x_{i-1/2}$. The spatial derivatives up to K th order at cell boundary

$$\begin{aligned} \overline{D_x^{(k)} \phi}_{i \pm \frac{1}{2}} &= \frac{\partial^k \phi}{\partial x^k}(x_{i \pm \frac{1}{2}}, t) \equiv \partial_x^{(k)} \phi; \\ &\text{with } k = 0, 1, \dots, K; \end{aligned} \quad (2)$$

are also used as the moments. Note that the point value (PV) $\overline{\phi}_{i+1/2}$ is actually equivalent to the 0th derivative moment $\overline{D_x^{(0)} \phi}_{i+1/2}$. We will denote the k th derivative of ϕ in respect to any variable β , $\partial^k \phi / \partial \beta^k$, by $\partial_\beta^{(k)} \phi$ occasionally hereafter.

Given one VIA $\overline{\phi}_i$ and $2(K+1)$ derivative moments $\overline{D_x^{(k)} \phi}_{i \pm \frac{1}{2}}$ over $[x_{i-1/2}, x_{i+1/2}]$, as well as the first-order derivative or gradient d_i that is computed in terms of other independent moments, we can construct a $[2(K+1)+1]$ th order cell-wise polynomial $\Phi_i(x, t)$ with $2(K+2)$ constrained conditions as follows,

$$\int_{x_{i-1/2}}^{x_{i+1/2}} \Phi_i(x, t) dx = \overline{\phi}_i, \quad (3)$$

$$\partial_x^{(k)} \Phi_i(x_{i+1/2}) = \overline{D_x^{(k)} \phi}_{i+1/2}, \quad k = 0, 1, \dots, K; \quad (4)$$

$$\partial_x^{(k)} \Phi_i(x_{i-1/2}) = \overline{D_x^{(k)} \phi}_{i-1/2}, \quad k = 0, 1, \dots, K; \quad (5)$$

$$\partial_x^{(1)} \Phi_i(x_i) = d_i. \quad (6)$$

Thus, the piecewise interpolation polynomial,

$$\Phi_i(x) = \sum_{k=0}^K a_k (x - x_{i-1/2})^k, \quad k = 0, 1, \dots, K \quad (7)$$

is constructed over cell i . All the coefficients a_k can be uniquely computed from (3),(4),(5) and (6). The first-order derivative or gradient of the interpolation function d_i can be approximated in terms of the known moments. For example, a $[2(K+1)+1]$ th order polynomial is obtained if we specify $d_i = \partial_x^{(1)} \tilde{\Phi}_i(x_i)$ with $\tilde{\Phi}_i(x)$ is computed from constraint conditions (3), (4) and (5). Furthermore, a slope limiting can be imposed to d_i to suppress the numerical oscillation (see [15] for details). We used a single-cell minmod limiter in this paper.

It is obvious that the reconstruction discussed above can have a $2(K+1)$ th order accuracy for smooth solutions.

3. The scalar conservation laws

In this section, we consider the scalar conservative law as follows,

$$\frac{\partial \phi}{\partial t} + \frac{\partial f(\phi)}{\partial x} = 0, \quad (8)$$

where ϕ is the scalar state variable and $f(\phi)$ is the flux function. Assuming the hyperbolicity, we have a real characteristic velocity, $u = \partial_\phi^{(1)} f(\phi)$.

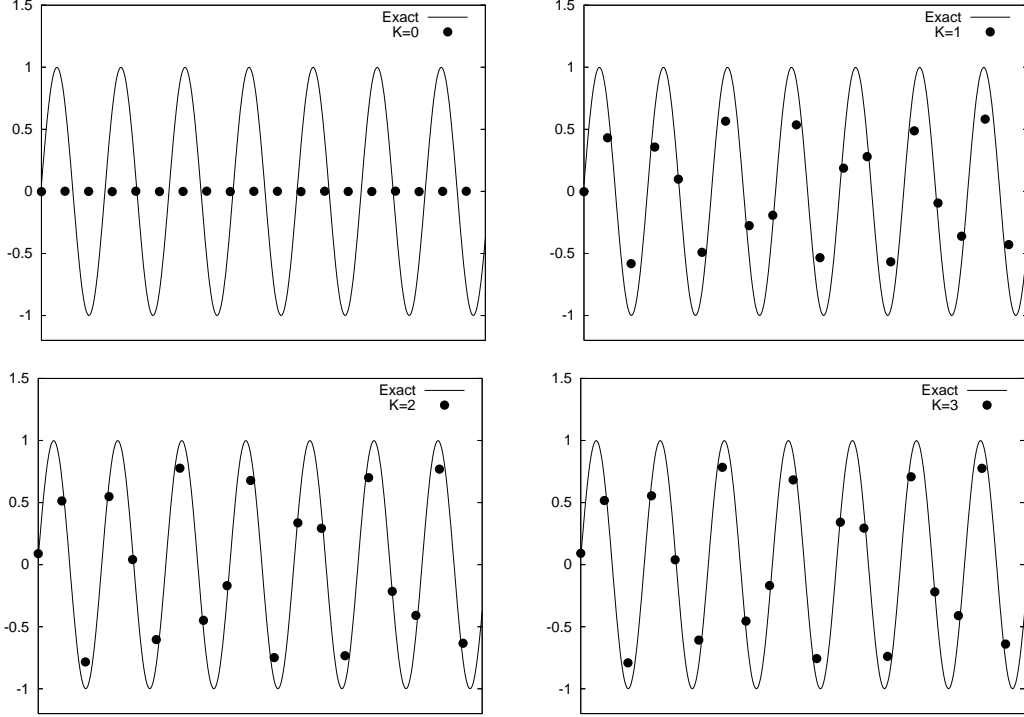


Figure 1: Advection transport of a harmonic wave after 400 steps (CFL=0.1) by schemes with derivative moments of 0th order (top-left), 1th order (top-right), 2nd order (bottom-left) and 3rd order (bottom-right).

The governing equations for the derivative moments can be directly derived from (8) as,

$$\partial_t^{(k)} \left(\overline{D_x^{(k)} \phi}_{i+\frac{1}{2}} \right) = -\partial_x^{(k+1)} \left(\hat{f} \overline{D_x^{(k)} \phi} \right)_{i+\frac{1}{2}}, \quad (9)$$

$$k = 0, 1, \dots, K;$$

where \hat{f} is the numerical flux function consistent to f .

It is observed from the reconstruction that the derivatives moments up to the K th order $\overline{D_x^{(k)} \phi}$ and flux $\partial_x^{(k)} \hat{f}$ are continuous. Thus, we can update the derivative moments $\overline{D_x^{(k)} \phi}_{i+\frac{1}{2}}$ for $k = 0, 1, \dots, K-1$ by (10) with the spatial derivatives of the flux function $\partial_x^{(k)} \hat{f}_{i+\frac{1}{2}}$ directly computed from the derivative moments that readily defined and computed at the cell interface as

$$\partial_x^{(k)} \hat{f}_{i+\frac{1}{2}} = \partial_x^{(k)} f(\overline{D_x^{(0)} \phi}_{i+\frac{1}{2}}, \overline{D_x^{(1)} \phi}_{i+\frac{1}{2}}, \dots, \overline{D_x^{(K)} \phi}_{i+\frac{1}{2}}). \quad (10)$$

When one advances the highest order derivative moment $\overline{D_x^{(K)} \phi}$, $\partial^{(K+1)} \hat{f} / \partial x^{K+1}$ is required, which, however, might not be continuous at the cell boundaries. We make use the the simple Lax-Friedrichs splitting in terms of the spatial derivatives of the flux function and the state variable as

$$\begin{aligned} \partial_x^{(K+1)} \hat{f}_{i+\frac{1}{2}} = & \quad (11) \\ & \frac{1}{2} \left(\partial_x^{(K+1)} \hat{f}(\phi^L)_{i+\frac{1}{2}} + \partial_x^{(K+1)} \hat{f}(\phi^R)_{i+\frac{1}{2}} \right) \\ & - \frac{\alpha_{i+\frac{1}{2}}}{2} \left(\partial_x^{(K+1)} \phi_{i+\frac{1}{2}}^L - \partial_x^{(K+1)} \phi_{i+\frac{1}{2}}^R \right), \end{aligned}$$

where $\alpha_{i+\frac{1}{2}}$ is the largest value of the characteristic speed in the related region.

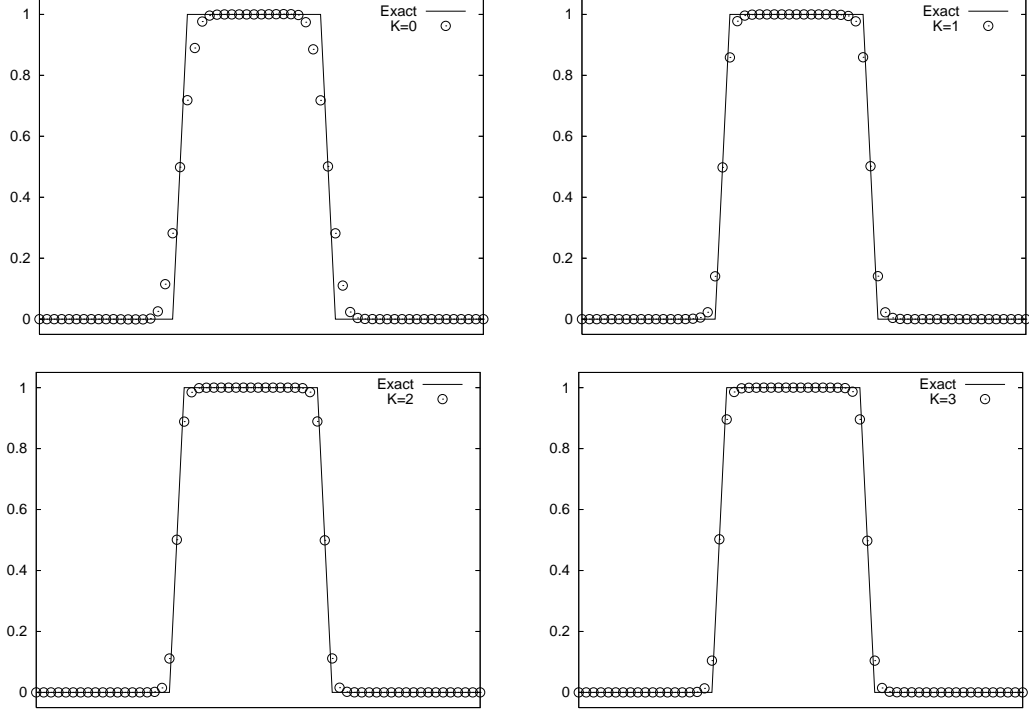


Figure 2: Advection transport of a square pulse after 2000 steps (CFL=0.1) by schemes with derivative moments of 0th order (top-left), 1th order (top-right), 2nd order (bottom-left) and 3rd order (bottom-right).

The state variables $\phi_{i+\frac{1}{2}}^L$ and $\hat{\phi}_{i+\frac{1}{2}}^R$ are computed from the multi-moment reconstructions (7) separately built for cells $[x_{i-1/2}, x_{i+1/2}]$ and $[x_{i+1/2}, x_{i+3/2}]$, i.e.

$$\phi_{i+\frac{1}{2}}^L = \Phi_i(x_{i+\frac{1}{2}}) \quad \text{and} \quad \phi_{i+\frac{1}{2}}^R = \Phi_{i+1}(x_{i+\frac{1}{2}}).$$

The corresponding $(K + 1)$ derivatives are

$$\partial_x^{(K+1)} \phi_{i+\frac{1}{2}}^L = \partial_x^{(K+1)} \Phi_i(x_{i+\frac{1}{2}}) \quad \text{and} \quad (12)$$

$$\partial_x^{(K+1)} \phi_{i+\frac{1}{2}}^R = \partial_x^{(K+1)} \Phi_{i+1}(x_{i+\frac{1}{2}}). \quad (13)$$

It should be noted that we have used an assumption similar to [9][10][11] in getting a homogeneous and linearized Riemann problem for spatial derivatives for the state variable.

In order to update the VIA moment, we integrate (8) over $[x_{i-1/2}, x_{i+1/2}]$, yielding the following conservative formulation,

$$\frac{\partial \bar{\phi}_i}{\partial t} = -\frac{1}{\Delta x_i} (\mathcal{F}(\bar{D}_x^{(k)} \phi_{i+\frac{1}{2}}) - \mathcal{F}(\bar{D}_x^{(k)} \phi_{i+\frac{1}{2}})), \quad (14)$$

where \mathcal{F} denotes the numerical flux at cell boundary, and is computed directly from the derivative moments readily updated at the cell boundaries.

The semi-discretized time evolution equations (9) and (14) are predicted in time by a TVD[6] or a 4th order Runge-Kutta method. At every substep, we first update the derivative moments by (9), and then use these updated moments to evaluate the flux function in (14).

We computed an advected harmonic wave with a wavelength of $20/7\Delta x$. Fig.1 shows the results for reconstructions using derivatives moments up to different orders. It is found that even a short wave can be adequately resolve if higher order derivative moments are used.

Fig.2 reveals the effect of limiting. The numerical oscillation associating discontinuities are eliminated by the slope switching that is also constructed within a single mesh element.

4. The Euler conservation laws

In this section, the numerical formulation presented above is implemented to the inviscid Euler conservation laws. The conservative form of the one-dimensional Euler equations is written as follows,

$$\frac{\partial \mathbf{U}}{\partial t} + \frac{\partial \mathbf{F}}{\partial x} = 0, \quad \mathbf{U} = \begin{pmatrix} \rho \\ \rho u \\ e \end{pmatrix}, \quad \mathbf{F} = \begin{pmatrix} \rho u \\ \rho u^2 + p \\ u(e + p) \end{pmatrix}, \quad (15)$$

where \mathbf{U} is the vector of conservative variables and \mathbf{F} is the vector of inviscid fluxes. Denoted by ρ is the density, u the velocity, e the total energy and p the pressure that is obtained by the equation of state for the perfect gas $p = (e - \rho u^2/2)(\gamma - 1)$. The ratio of the specific heats γ is specified as 1.4 in this paper.

The volume-integrated average (VIA) moment over mesh cell i ,

$$\overline{\mathbf{U}}_i = \frac{1}{\Delta x_i} \int_{x_{i-\frac{1}{2}}}^{x_{i+\frac{1}{2}}} \mathbf{U}(x, t) dx, \quad (16)$$

and the derivative moments up to K th order at cell boundary,

$$\overline{D_x^{(k)} \mathbf{U}}_{i+\frac{1}{2}} = \frac{\partial^k \mathbf{U}}{\partial x^k}(x_{i+\frac{1}{2}}, t) \quad \text{with } k = 0, 1, \dots, K; \quad (17)$$

are treated as the model variables.

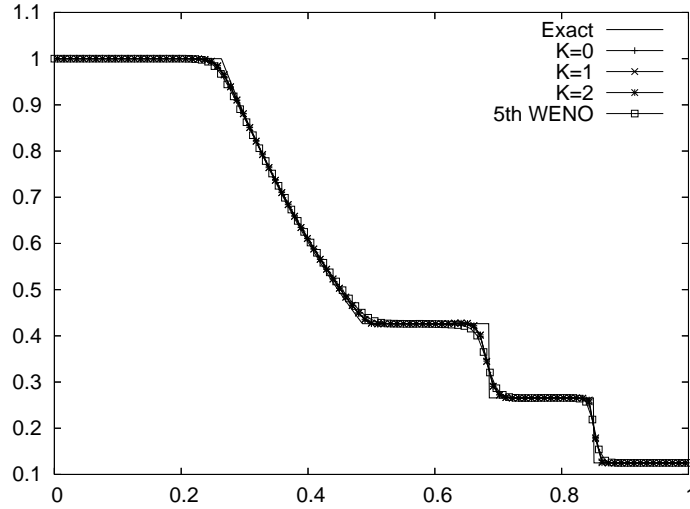


Figure 3: Numerical results of Sod's problem at $t = 0.2$ separately computed by the multi-moment reconstructions with $K = 0, 1, 2$ and the 5th-order WENO scheme are plotted.

Analogous to the scalar case, the governing equations for the derivative moments are derived from (15) as,

$$\begin{aligned} \partial^{(k)}_t \left(\overline{D_x^{(k)} \mathbf{U}}_{i+\frac{1}{2}} \right) = \\ - \partial_x^{(k+1)} \left(\hat{\mathbf{F}}(\overline{D_x^{(k)} \mathbf{U}}) \right)_{i+\frac{1}{2}}, \quad k = 0, 1, \dots, K; \end{aligned} \quad (18)$$

where $\hat{\mathbf{F}}$ is the vector of the numerical flux function consistent to \mathbf{F} .

Given $\overline{D_x^{(k)}\mathbf{U}}_{i+\frac{1}{2}}$ continuous for $k = 0, 1, \dots, K$, we can update the derivative moments $\overline{D_x^{(k)}\mathbf{U}}_{i+\frac{1}{2}}$ for $k = 0, 1, \dots, K-1$ by (19) with the spatial derivatives of the flux function $\partial_x^{(k)}\hat{\mathbf{F}}$ evaluated directly from

$$\begin{aligned} (\partial_x^{(k)}\hat{\mathbf{F}})_{i+\frac{1}{2}} = \\ \partial_x^{(k)}\hat{\mathbf{F}}(\overline{D_x^{(0)}\mathbf{U}}_{i+\frac{1}{2}}, \overline{D_x^{(1)}\mathbf{U}}_{i+\frac{1}{2}}, \dots, \overline{D_x^{(k)}\mathbf{U}}_{i+\frac{1}{2}}). \end{aligned} \quad (19)$$

Similar to the scalar case, $\partial_x^{(K+1)}\hat{\mathbf{F}}$ might be not continuous at the cell boundaries. So, the highest order derivative moment $\overline{D_x^{(K)}\mathbf{U}}$ has to be solved from a Riemann problem in terms of the spatial derivative. To this end, we use the linearization assumption in [9][10] and write the $(K+1)$ th spatial derivative of the flux function as

$$\partial_x^{(K+1)}\mathbf{F} = \mathbf{A}\partial_x^{(K)}\mathbf{U}, \quad (20)$$

where \mathbf{A} is the Jacobian matrix.

The conventional flux splitting algorithms can be adopted here in terms of the spatial derivative quantities.

The $(K+1)$ th derivatives of the state variables and the flux function at the cell interface are computed from the multi-moment reconstructions separately built over two neighboring cells as (12) and (13) component-wisely in terms of the the state variables or characteristic variables.

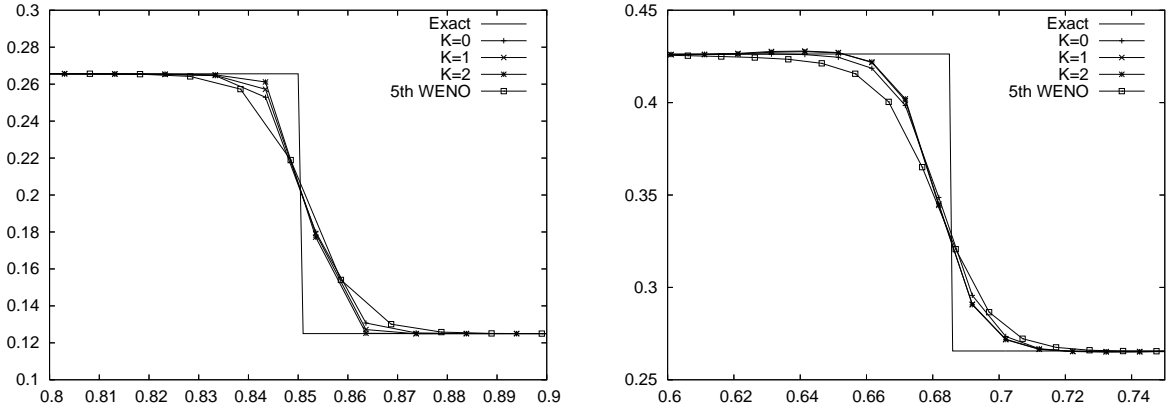


Figure 4: The close-up views for shock (left) and contact discontinuity(right).

The VIAs of the conservative variables \mathbf{U} on cell i are updated by integrating (15) over $[x_{i-1/2}, x_{i+1/2}]$, which results in a finite volume formulation,

$$\frac{\partial \overline{V\mathbf{U}}}{\partial t}_i = -\frac{1}{\Delta x_i} \left(-\hat{\mathbf{F}}(\overline{D_x^{(k)}\mathbf{U}}_{i+\frac{1}{2}}) - \hat{\mathbf{F}}(\overline{D_x^{(k)}\mathbf{U}}_{i+\frac{1}{2}}) \right). \quad (21)$$

Given the derivative moments $\overline{D_x^{(k)}\mathbf{U}}_{i+\frac{1}{2}}$ at cell boundaries, the numerical fluxes $\hat{\mathbf{F}}(\overline{D_x^{(k)}\mathbf{U}}_{i+\frac{1}{2}})$ in the above equation are directly found.

Again, the Runge-Kutta method is used for time integration for all moments.

A 1D shock tube test[7] was computed to verify the present method for Euler conservation laws. We include the numerical result of the 5th-order WENO scheme[5] as well for comparison. Shown in Fig.3, the numerical results of the present scheme with different orders are quite competitive. The close-up plots for shock and contact discontinuity are given in Fig.4. Both linear and non-linear discontinuities are well resolved with correct locations. It is observed that better resolution can be obtained by simply increasing the order of the derivative moments.

5. Concluding remarks

A formulation that uses high order derivative moments has been suggested and tested. Given all the derivative moments that are continuous at cell boundaries and updated separately, the resulting numerical formulation is still single-cell based and quite computationally efficient. In case that the derivative moments are defined and continuous at the cell boundary, the numerical fluxes can be computed directly as in the IDO scheme [1], while for the spatial derivative higher than the continuous one, we simplify and cast it into a linearized derivative Riemann problem[9]. The present formulation is substantially different from the ADER method[9][10] [11] where all the derivatives are discontinuous at cell boundaries, thus is more efficient.

Our numerical results show that the resolution of the scheme can be improved by simply increasing the order of the derivative moments involved. With the simple slope limiting[15], the numerical oscillation around the large gradient can be effectively suppressed.

Although the multi-dimension implementation remains an open problem to be further explored, one can expect the present scheme as an accurate efficient solver for 1D conservation laws.

References

- [1] T. Aoki, Comput. Phys. Commun. **102** (1997) 132.
- [2] A. Harten, B. Engquist, S. Osher and S. Chakravarthy, J. Comput. Phys. **71** (1987) 231.
- [3] S. Ii, M. Shimuta and F. Xiao, Comput. Phys. Comm. **173** (2005) 17.
- [4] S. Ii and F. Xiao, J. Comput. Phys. **222** (2007) 849.
- [5] G. Jiang and C.W. Shu, J. Comput. Phys. **126** (1996) 202.
- [6] C.W. Shu, SIAM J. Sci. Stat. Comput. **9** (1988) 1073.
- [7] G. Sod, J. Comput. Phys. **27** (1978) 1.
- [8] R. Tanaka, T. Nakamura and T. Yabe, Comput. Phys. Commun. **126** (2000) 232.
- [9] V.A.Titarev and E.F.Toro, J. Sci. Comput. **17** (2002) 609.
- [10] V.A.Titarev and E.F.Toro, J. Comput. Phys. **204** (2005) 715.
- [11] E.F.Toro and V.A.Titarev, J. Comput. Phys. **202** (2005) 196.
- [12] B. van Leer, J. Comput. Phys. **32** (1979) 101.
- [13] F. Xiao, J. Comput. Phys. **195** (2004) 629.
- [14] F. Xiao, R. Akoh and S. Ii, J. Comput. Phys. **213** (2006) 31.
- [15] F. Xiao and T. Yabe, J. Comput. Phys. **170** (2001) 498.
- [16] T. Yabe and T. Aoki, Comput. Phys. Commun. **66** (1991) 219.